JOURNAL OF THE AMERICAN CHEMICAL SOCIETY

Subscriber access provided by Northern Illinois University

Communication

Substituent Directed Photo-Transformations of BN-Heterocycles: Elimination vs Isomerization via Selective B-C Bond Cleavage

Deng-Tao Yang, Soren K Mellerup, Jin-Bao Peng, Xiang Wang, Quan-Song Li, and Suning Wang

J. Am. Chem. Soc., **Just Accepted Manuscript** • DOI: 10.1021/jacs.6b07899 • Publication Date (Web): 31 Aug 2016

Downloaded from http://pubs.acs.org on August 31, 2016

Just Accepted

“Just Accepted” manuscripts have been peer-reviewed and accepted for publication. They are posted online prior to technical editing, formatting for publication and author proofing. The American Chemical Society provides “Just Accepted” as a free service to the research community to expedite the dissemination of scientific material as soon as possible after acceptance. “Just Accepted” manuscripts appear in full in PDF format accompanied by an HTML abstract. “Just Accepted” manuscripts have been fully peer reviewed, but should not be considered the official version of record. They are accessible to all readers and citable by the Digital Object Identifier (DOI®). “Just Accepted” is an optional service offered to authors. Therefore, the “Just Accepted” Web site may not include all articles that will be published in the journal. After a manuscript is technically edited and formatted, it will be removed from the “Just Accepted” Web site and published as an ASAP article. Note that technical editing may introduce minor changes to the manuscript text and/or graphics which could affect content, and all legal disclaimers and ethical guidelines that apply to the journal pertain. ACS cannot be held responsible for errors or consequences arising from the use of information contained in these “Just Accepted” manuscripts.

ACS Publications

Journal of the American Chemical Society is published by the American Chemical Society. 1155 Sixteenth Street N.W., Washington, DC 20036

Published by American Chemical Society. Copyright © American Chemical Society. However, no copyright claim is made to original U.S. Government works, or works produced by employees of any Commonwealth realm Crown government in the course of their duties.

Substituent Directed Photo-Transformations of BN-Heterocycles: Elimination *vs* Isomerization *via* Selective B-C Bond Cleavage

Deng-Tao Yang,[†] Soren K. Mellerup,[†] Jin-Bao Peng,[†] Xiang Wang,[†] Quan-Song Li,*[‡] and Suning Wang*[†‡]

[†]Department of Chemistry, Queen's University, Kingston, Ontario K7L 3N6, Canada

[‡]Beijing Key Laboratory of Photoelectronic/Electrophotonic Conversion Materials, School of Chemistry, Beijing Institute of Technology, Beijing 100081, P. R. China

Supporting Information Placeholder

ABSTRACT: Electron-rich and electron-poor BN-heterocycles with benzyl-pyridyl chelate backbones and two bulky aryl groups on the boron center (Ar = tipp, **BN-1**, Ar = MesF, **BN-2**) have been found to display distinct molecular transformations upon irradiation by UV light. **BN-1** undergoes an exceptionally efficient photoelimination reaction forming a BN-phenanthrene (**BN-phen-1**) with Φ_{PE} = 0.25, while **BN-2** undergoes a thermally reversible, stereoselective, and quantitative isomerization to a dark colored BN-1,3,5-cyclooctatriene (BN-1,3,5-COT, **BN-2a**). This unusual photoisomerization persists for other BN-heterocycles with electron-deficient aryl groups such as **BN-3** with a benzyl-benzothiazolyl backbone and Mes^F substituents or **BN-4** with a benzyl-pyridyl backbone and two C_6F_5 groups on the boron center. The photoisomerization of **BN-4** goes beyond BN-1,3,5-COT (**BN-4a**), forming a new BN-1,3,6-cyclooctatriene species (BN-1,3,6-COT, **BN-4b**) *via* C–F bond cleavage and [1,3]-F atom sigmatropic migration. DFT and TD-DFT mechanistic studies support that **BN-4a** is an intermediate in the formation of **BN-4b**. This work establishes that steric and electronic factors can effectively control the molecular transformations of BN-heterocycles, allowing access to important and previously unknown BN-embedded species.

Controlling the fate of chemical transformations is one of the cornerstones of modern chemistry and biology. While nature has achieved this feat by employing complicated and unique molecular architectures (*e.g.* enzymes),[1] chemists rely heavily on manipulating the steric and electronic factors of small molecules/complexes[2] to promote desired reaction outcomes. For example, steric/electronic considerations have proven highly effective in both the stabilization of rare chemical entities[3] as well as the facilitation of unique molecular transformations.[4] Recently, similar strategies have been applied to organoboron systems, which has demonstrated the remarkable breadth of varying reactivity and functions available to these species[5] (*e.g.* optoelectronics,[5b-h] catalytic components,[5i-l] organic synthons,[5m-q] *etc*). To this end, we have had a long-standing interest in the photo-responsive properties of organoboron compounds,[6,7] where we have previously shown that BN-heterocycles such as **BN-0** (R = Me, X = H; Scheme 1) are capable of undergoing photoelimination of mesitylene to produce fully conjugated and highly luminescent BN-phenanthrenes (**BN-phen**).[6d] While this transformation does provide a new method of preparing these BN-phenanthrene isomers and allow for the *in-situ* generation of optoelectronic devices such as OLEDs based on such BN-systems,[7] the low quantum efficiency of the photoreaction ($\Phi_{PE} \leq 0.044$) severely limits its synthetic and practical usefulness. Inspection of the DFT-calculated transition state for this reaction revealed that B–C_{Ar} bond breaking is likely the rate-limiting step.[6f,g] Therefore, we postulated that weakening the B–C_{Ar} bond through either greater steric encumberment, *i.e.* replacing the Mes groups in **BN-0** with 2,4,6-triisopropylphenyl (tipp, **BN-1**) or bulky/strongly electron-withdrawing groups such as 2,4,6-trifluoromethylphenyl (Mes^F, **BN-2**), could improve the efficiency of the photoelimination. Indeed, this strategy proved successful with respect to **BN-1**, which eliminated much more efficiently than **BN-0**. Remarkably, however, instead of elimination **BN-2** exhibited an unprecedented photochromic switching around the boron core, generating an intensely colored and previously unknown BN-1,3,5-cyclooctatriene (COT). Further investigation revealed that the photochemical formation of BN-1,3,5-COT is a general phenomenon for BN-heterocycles that contain electron-deficient aryl groups on boron, thus establishing the possibility to control such molecular transformations by tuning the steric and electronic properties of the molecule. The details of the two distinct phototransformations and mechanistic insights are presented herein.

Scheme 1. Substituent-Directed Transformations of BN-heterocycles

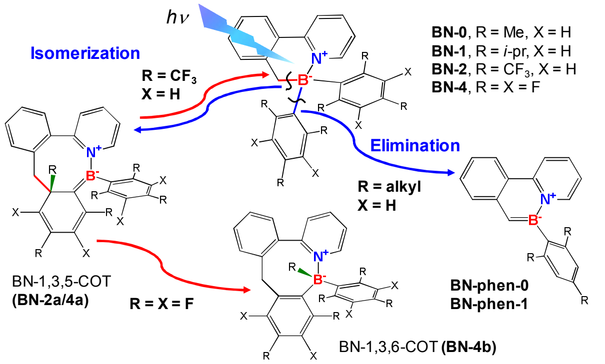

Compounds **BN-1** and **BN-2** were prepared using a modified procedure[6d] reported previously for **BN-0** and the corresponding *in-situ* generated Ar_2BX (X = F, Cl) reagents. Both were fully characterized by ^1H, ^{13}C, ^{11}B, and ^{19}F NMR, HRMS, and single crystal X-ray diffraction analyses (Figure 1). Crystal data revealed that the B–C_{Ar} bonds of **BN-1** and **BN-2** are about 0.02 Å longer than those of **BN-0**, while all three B-CH_2 bond lengths are comparable. The DFT-calculated B–C_{Ar} lengths match well with those determined experimentally, with the calculated B-Mes^F lengths in **BN-2** being ~0.01 Å longer than those of B-tipp in **BN-1**. This difference highlights the strong withdrawing nature of Mes^F in addition to its steric bulk.

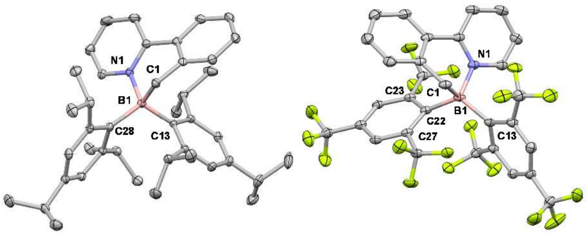

Figure 1. Crystal structure of **BN-1** (left) and **BN-2** (right). Key bond lengths (Å) for **BN-1**: B(1) – C(13)/C(28) 1.680(2)/1.682(2), B(1) – C(1)/N(1) 1.639(2)/1.684(2). For **BN-2**: B(1) – C(13)/ C(22) 1.681(3)/1.689(2), B(1) – C(1)/N(1) 1.642(2)/1.636(2).

The photoreactivity of **BN-1** in solution and polymer films is similar to that of **BN-0**, with the brightly green fluorescent **BN-phen-1** (λ_{em} = 500 nm, Φ_{FL} = 0.27) formed quantitatively upon irradiation at 300 nm as evidenced by UV-Vis, NMR, and crystal structure data (see SI). The most striking difference between **BN-0** and **BN-1** is the rate of photoelimination. Because both compounds have identical absorption spectra and form similar products, the Φ_{PE} of **BN-1** relative to that of **BN-0** was determined to be 0.25 using competitive NMR photolysis experiments (see SI). The Φ_{PE} of **BN-1** is *ca.* 6 times greater than that of **BN-0** (0.044), exceptionally high for a photoelimination reaction, as they tend to have a very low Φ_{PE}. The weaker B-tipp bonds of **BN-1** are clearly responsible for this significant enhancement in photoelimination efficiency. This demonstrates that the use of bulkier electron rich aryl groups on boron is an effective strategy for achieving highly efficient aryl-elimination in such systems, thus making the use of BN-heterocycles as precursors for *in-situ* fabrication of azaborine-based optoelectronic devices[7] more viable.

Despite a similarly congested structure and long B-Mes^F bonds, **BN-2** does not undergo photoelimination at all. Irradiation (300 nm) of **BN-2** in C_6D_6 or THF resulted in the rapid and clean conversion of **BN-2** to a new species, **BN-2a**, which has sharp and well-resolved peaks in the ^1H NMR spectrum and a ^{11}B chemical shift at ~35 ppm, typical of a three-coordinated boron with one unsaturated bond[8] (Figure 2b and SI). Accompanying the NMR spectral change was a dramatic change in solution colour from colorless to dark orange-brown as shown in Figure 2. In the UV-Vis spectrum, a broad low energy absorption band at λ_{max} = 433 nm (Figure 2d) appears with irradiation. TD-DFT data suggests that the low energy band of **BN-2a** originates from a charge transfer (CT) transition from HOMO located on the π-system of the B=C and the cyclohexandiene moiety to LUMO (π*) located on the py ring of the backbone (see SI). Remarkably, heating the orange-brown solution at 90 °C resulted in full recovery of **BN-2** by NMR and restoration of the original solution colour. The activation energy of this process was determined to be ~33.3 kcal/mol (see SI). **BN-2a** forms dark orange-brown crystals, allowing us to establish its structure unequivocally by X-ray diffraction.

The crystal structure of **BN-2a** (Figure 3) revealed a previously unknown BN-embedded cyclic structure, which is formally a 4,5-dihydro-1,2-azaborocine but will be described as BN-1,3,5-cyclooctatriene (BN-1,3,5-COT) for convenience. The CH_2 group in **BN-2a** is no longer bound to the boron atom, but instead forms a C-C bond with one CF_3-substituted quaternary carbon atom (C(14)) of a Mes^F ring. This converts the Mes^F to a 1,3-cyclohexadiene and the B-C bond to a B=C bond (1.465(3) Å), with similar length compared to previously reported B=C bonds.[8] Comparing the structure of **BN-2a** to the photoproduct of previously reported B(ppy)Mes_2,[6a-6d] which forms a tricyclic 1,2-azaboratabisnorcaradiene, it is clear that the switching described for **BN-2** represents a brand new class of photochromic materials. The Φ_{PE} of **BN-2** to **BN-2a** transformation was determined to be 0.23 (see SI). BN-1,3,5-COTs are a previously unknown class of BN-embedded molecules. The clean and quantitative generation of **BN-2a** *via* the photoisomerization of **BN-2** provides a convenient method for accessing such unusual species. Furthermore, despite **BN-2a** having a chiral carbon atom (C(14)) and chiral COT structure, only one diastereoisomer was observed by NMR in which the CF_3 (C(19)) is *syn* to the py ring while the phenyl and the cyclohexadienyl of the COT unit are *syn* to each other. Thus, the **BN-2** to **BN-2a** transformation proceeds with high stereoselectivity.

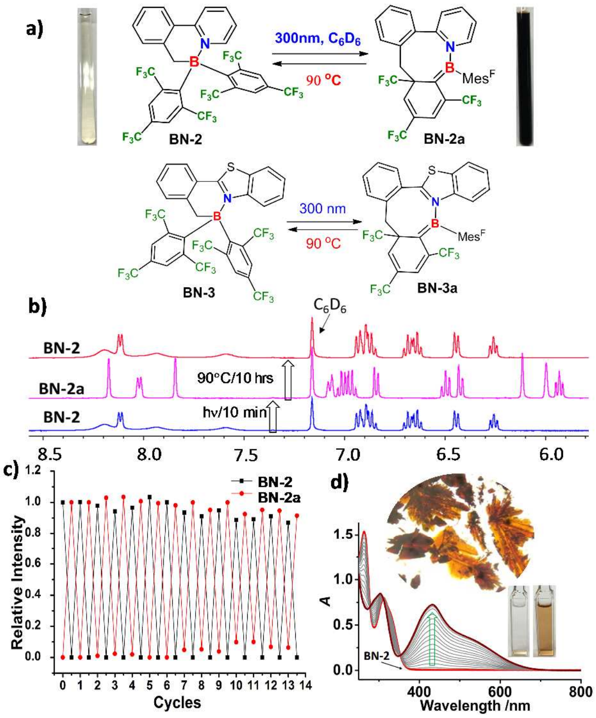

Figure 2. a) A scheme showing the interconversion of **BN-2**/**BN-3** and **BN-2a**/**BN-3a**. b) ^1H NMR spectra showing the photo (300 nm) and thermal (90 °C) interconversion of **BN-2** and **BN-2a** in C_6D_6. c) A diagram showing the fatigue resistance of the **BN-2** and **BN-2a** with the irradiation and heating cycles using integrated peak intensity relative to the C_6D_6 peak in ^1H NMR spectra (see Fig. S3.3). d) UV-Vis spectra showing the conversion of **BN-2** to **BN-2a** in THF (1×10^{-4} M) and photographs showing the crystals of **BN-2a** and solution color of **BN-2** and **BN-2a**.

To demonstrate the robustness of this newly discovered photochromic system, the fatigue resistance of **BN-2** was examined by cycling through the **BN-2→BN-2a→BN-2** transformations repeatedly. Quite remarkably, the continuous photo-thermal cycling between these two states did not yield any appreciable decomposition until the 13th cycle as shown by ^1H NMR data (Figure 2c and SI), indicating that **BN-2**/**BN-2a** possess excellent fatigue resistance. This feature makes these systems promising for future applications involving molecular switches.

To establish if the new photo-transformation is available to other BN-heterocycles with different chelate backbones, **BN-3**, an analogue of **BN-2** with a 2-benzyl-benzothiazolyl backbone was prepared (Figure 2). Upon irradiation at 300 nm, **BN-3** undergoes a similar photo-switching as observed for **BN-2** (see SI), forming a deep brown colored **BN-3a**, an analogue of **BN-2a**, according to its diagnostic ^{1}H, ^{11}B, and ^{19}F NMR spectra. Again, only one diastereoisomer was observed. **BN-3a** possesses a low energy absorption band with λ_{max} = 458 nm in its UV-Vis spectrum, which is red-shifted by ~25 nm compared to **BN-2a**, consistent with the greater π-conjugation of the backbone in **BN-3a**. The Φ_{PE} of **BN-3** to **BN-3a** transformation was determined to be 0.10. Thermally, **BN-3a** converts back to the colorless **BN-3** at 90 °C with ~5% decomposition observed in the process (see SI). This example shows that the new photochromic phenomenon is not limited to systems with a benzyl-pyridyl backbone.

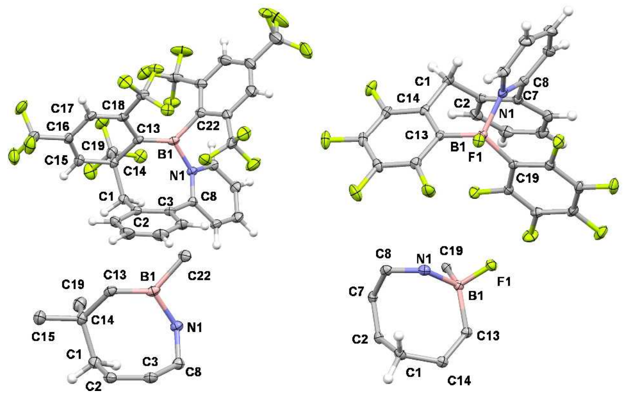

Figure 3. Crystal structures of **BN-2a** (left), **BN-4b** (right), and the BN-COT cores. Important bond lengths (Å) for **BN-2a**: B(1) – C(13)/C(22)/N(1) 1.465(3)/1.627(3)/1.585(3), C(8) – N(1)/C(3) 1.372(2)/1.477(3), C(2) – C(1)/C(3) 1.498(3)/1.390(3); C(14) – C(1)/C(13)/C(15)/C(19) 1.567(3)/1.564(3)/1.509(3)/1.528(3), C(16) – C(15)/C(17) 1.322(3)/1.427(3), C(18) – C(13)/C(17) 1.461(3)/1.352(3). For **BN-4b**: B(1)–F(1)/N(1)/C(13)/C(19) 1.408(2)/1.658(2)/1.628(2)/1.636(2), C(8) – N(1)/C(7) 1.356(2)/1.480(2); C(2) – C(1)/C(7) 1.510(2)/1.397(2), C(14) – C(1)/C(13) 1.514(2)/1.408(2).

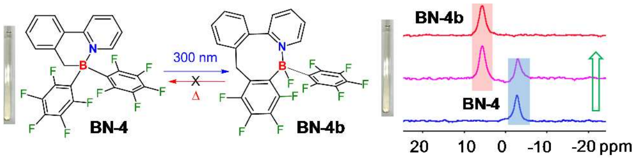

Figure 4. Irreversible photoisomerization of **BN-4** and the ^{11}B NMR spectra in C_6D_6 showing the full conversion of **BN-4** (blue) to **BN-4b** (red).

Given the bulky nature of the aryl groups in **BN-1**, **BN-2**, and **BN-3**, but their distinctly different photoreactivity, the electron-deficiency of Mes^{F} appears to be pivotal for the new photochromism. To probe this hypothesis, the photoreactivity of **BN-4**,[6f] which has the same backbone as **BN-2** and two less sterically congested but comparably electron-withdrawing C_6F_5 substituents, was examined. Upon irradiation of **BN-4** at 300 nm, no obvious color change was observed. However, ^{1}H, ^{19}F, and ^{11}B NMR revealed the quantitative formation of a new species, **BN-4b**, with a typical four-coordinated ^{11}B chemical shift of 5.6 ppm (Figure 4 and SI). Single-crystal X-ray diffraction analysis established that **BN-4b** shares some structural similarities with **BN-2a**/**3a** and may be described as a BN-embedded 1,3,6-COT, an isomer of BN-1,3,5-COT, as shown in Figure 3. The key difference between **BN-2a**/**3a** and **BN-4b** is that the 3rd double bond in the latter is not conjugated with the other two in the COT ring, and the boron center is four-coordinated with a B-F bond. As a consequence, **BN-4b** has no low energy absorption band in the visible region, which is consistent with TD-DFT calculated data (see SI). The B atom in **BN-4b** is a chiral center, which, combined with the chiral COT structure, creates the possibility of diastereomers. The fact that only one diastereomer was observed in which the B-F bond is *syn* to the py ring as shown in Figure 3 supports that the **BN-4** to **BN-4b** transformation also has high stereoselectivity. Unlike **BN-2a/3a** which can thermally revert to **BN-2/3**, **BN-4b** is thermally stable and does not convert back to **BN-4**. Given the bond energy of the C-F bond,[9] its cleavage in the **BN-4** to **BN-4b** transformation is highly unusual and interesting, which may be driven by the stability of **BN-4b**.

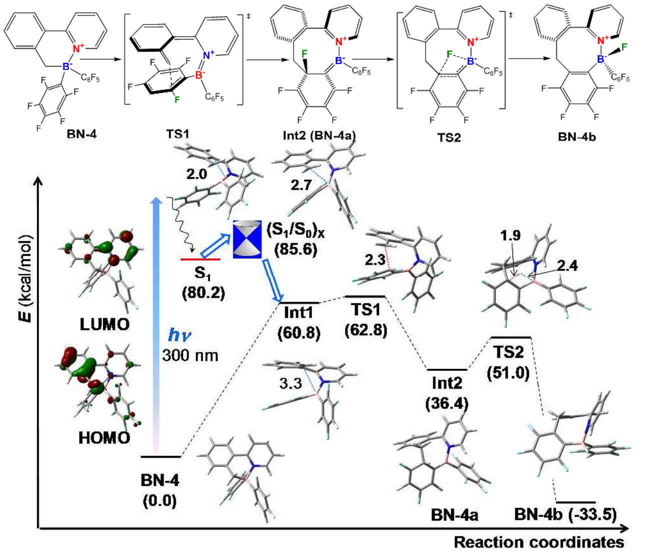

Figure 5. Calculated potential energy profile for the photoisomerization of **BN-4**. The energies of the all key species, as well as the intersection point of the S_0 and S_1 state ($(S_1/S_0)_X$) are relative to **BN-4** and given in the parentheses. Some key distances (in Å) and the HOMO/LUMO orbitals of **BN-4** are also shown.

To understand the unusual photoisomerization of **BN-2**/**4**, DFT and TD-DFT calculations were performed for each with the complete reaction pathway of **BN-4** shown in Figure 5. Excitation at 300 nm populates the S_1 state of **BN-4** at the Franck-Condon (FC) structure, which is of ππ* character and mainly arises from its HOMO to LUMO transition. Relaxation leads to a minimum in the S_1 state, which is close in energy (~5 kcal mol^{-1}) to a conical intersection point $(S_1/S_0)_X$ between the S_1 and S_0 states, therefore allowing access to the ground state from the excited state.[10] In the S_0, S_1, and $(S_1/S_0)_X$ structures, the B-CH$_2$ distances are 1.6, 2.0, and 2.7 Å, respectively, indicating that the B-CH$_2$ is broken upon photo-excitation. At $(S_1/S_0)_X$, the excited state decays to the ground state and the reaction path leads to an intermediate (Int1) with a B-CH$_2$ distance of 3.3 Å, a negatively charged (-0.44 e) CH$_2$ carbon atom, and a positively charged (+0.29 e) *o*-carbon of one C_6F_5 ring. The latter two moieties have a separation distance of 2.3 Å at the TS1 state, with perfect orientation for C-C bond formation or electrocyclization similar to that observed in a photochromic boron system reported by Yamaguchi,[11] generating Int2 (**BN-4a**), an analogue of **BN-2a**. The TS1 state lies only 2 kcal/mol above Int1, suggesting that the reaction from Int1 to **BN-4a** occurs readily. Unlike **BN-2a**, which does not undergo further isomerization, the F atom of **BN-4a** can migrate from carbon to boron by overcoming a barrier of ~15 kcal/mol at the TS2 state forming **BN-4b**, which resembles the classic transition state structure proposed for 1,3-sigmatropic shifts, leading to the selective formation of one diastereoisomer.[9c] The attraction between the F atom and the electron deficient B atom clearly favors the rearrangement from **BN-4a** to **BN-4b**, which is -33.5 kcal/mol lower in energy than **BN-4**. These data support that the formation of

BN-4b is thermodynamically favorable and the reverse reaction is prohibited due to the large reverse barrier of 96.3 kcal/mol. Due to the large size of **BN-2** and its analogous isomerization pathway, only the ground-state reaction pathway was determined. The key transition state of **BN-2** has a similar TS1 structure as **BN-4**, with the C-C distance between CH_2 and C_{CF3} being 2.4 Å (see SI). The calculated barrier for **BN-2a** reverting back to **BN-2** is 34.2 kcal/mol, which agrees very well with the experimental value of 33.3 kcal/mol. The fact that the BN-1,3,6-COT isomer was not observed for **BN-2** may be explained by an unfavorable transition state caused by steric crowding of the bulky CF_3 groups. The calculated reaction pathway also corroborates the stereoselective formation of **BN2a** and **BN-4b**.

One key feature revealed by DFT data is that the HOMO of **BN-2** and **BN-4** is localized mainly on the benzyl ring of the chelate backbone and the B atom with very little contributions from the Mes^F or C_6F_5 groups. This is in sharp contrast to **BN-0** and **BN-1**, in which the HOMO is made of almost exclusively π orbitals on the Mes and tipp groups (see Fig. S6.1e). The substituent groups on the aryl rings are clearly responsible for this distinct difference between the electron-rich and electron-poor BN-heterocycles, which led to their distinct photoreactivity (*i.e.* aryl-elimination *vs.* $-CH_2$ migration/isomerization). The electron-withdrawing Mes^F and C_6F_5 likely contribute to the stabilization of the TS1 state by strengthening the B=N bond. This stabilization effect by Mes^F substitution is reminiscent of that reported by Marder in borole systems[12a] and Jäkle in conjugated thienylborane systems[12b]. Further evidence to support the importance of electron-deficient aryl groups in the photoisomerization of BN-heterocycles are provided by the photostability of **BN-5** (replacing one C_6F_5 in **BN-4** by a phenyl ring) and **BN-6** (replacing both C_6F_5 in **BN-4** by two phenyl rings), which do not show any change under 300 nm irradiation for up to 48 hrs (see SI).

In summary, both electronic and steric effects have been found to have a significant and distinct impact on the photoreaction pathways of BN-heterocycles. With bulky, electron-donating aryl rings on the B atom, the photoelimination efficiency is greatly enhanced. In contrast, with sufficiently electron-withdrawing aryl groups on the B atom, bulky or not, photoisomerization occurs exclusively with high stereoselectivity. Bulky electron-withdrawing aryl groups such as Mes^F appear to be the key for reversible photo-thermal isomerization of this new class of photochromic molecules. Balancing steric and electronic factors is found to be critical for achieving the desired molecular transformations based on BN-heterocycles. The first examples of BN-1,3,5-COT and BN-1,3,6-COT molecules have been obtained and their relationship in structural transformation has been demonstrated.

ASSOCIATED CONTENT

Supporting Information

Spectroscopic data for new compounds, experimental and computational details, crystal structural data, and additional data. This material is available free of charge via the Internet at http://pubs.acs.org.

AUTHOR INFORMATION

Corresponding Author

wangs@chem.queensu.ca, liquansong@bit.edu.cn

Notes

The authors declare no competing financial interests.

ACKNOWLEDGMENT

The authors thank the Natural Science and Engineering Research Council of Canada (RGPIN1193993-2013) and the National Natural Science Foundation of China for Financial support (grants 21571017 and 21303007). S.K.M. thanks the Canadian Government for the Vanier Scholarship.

REFERENCES

(1) (a) *Microbial Enzymes and Biotechnology*; Fogarty, W. M., Kelly, C. T., Eds.; Springer Applied Science, New York, 2012, 2nd edition. (b) *Molybdenum and Molybdenum-Containing Enzymes*; Coughlan, M. P., Ed.; Pergamon Press, Willowdale, 1980. (c) *Immobilized Enzymes for Industrial Reactors*; Messing, R. A., Eds.; Academic Press, New York, 1975.

(2) (a) Grubbs, R. H.; Chang, S. *Tetrahedron* **1998**, *54*, 4413. (b) Schrock, R. R. *Tetrahedron* **1999**, *55*, 8141. (c) Anderson, J. S.; Rittle, J.; Peters, J. C. *Nature* **2013**, *501*, 804.

(3) (a) Braunschweig, H.; Dewhurst, R. D.; Schneider, A. *Chem. Rev.* **2010**, *110*, 3924. (b) Soleilhavoup, M.; Bertrand, G. *Acc. Chem. Res.* **2015**, *48*, 256. (c) Martin, C. D.; Soleilhavoup, M.; Bertrand, G. *Chem. Sci.* **2013**, *4*, 3020.

(4) (a) Berkovic, G.; Krongauz, V.; Weiss, V. *Chem. Rev.* **2000**, *100*, 1741 and references therein. (b) Irie, M. *Chem. Rev.* **2000**, *100*, 1685. (c) Ko, C.-C.; Yam, V. W.-W. *J. Mater. Chem.* **2010**, *20*, 2063.

(5) (a) *Boron Science New Technologies and Applications*; Hosmane, N. S., Eds.; CRC, Taylor & Francis, Boca Raton, 2012. (b) Entwistle, C. D.; Marder, T. B. *Chem. Mater.* **2004**, *16*, 4574. (c) Wakamiya, A.; Taniguchi, T.; Yamaguchi, S. *Angew. Chem. Int. Ed.* **2006**, *45*, 3170. (d) Chen, P.; Lalancette, R. A.; Jäkle, F. *Angew. Chem. Int. Ed.* **2012**, *51*, 7994. (e) Lorbach, A.; Hîbner, A.; Wagner, M. *Dalton Trans.* **2012**, *41*, 6048. (f) Escande, A. Ingleson, M. J. *Chem. Commun.* **2015**, *51*, 6257. (g) Wang, X.-Y.; Wang, J.-Y.; Pei, J. *Chem. Eur. J.* **2015**, *21*, 3528. (h) Li, D.; Zhang, H.; Wang, Y. *Chem. Soc. Rev.* **2013**, *42*, 8416. (i) Stephan, D. W. Erker, G. *Angew. Chem. Int. Ed.* **2015**, *54*, 6400. (j) McGough, J. S.; Butler, S. M.; Cade, I. A.; Ingleson, M. J. *Chem. Sci.* **2016**, *7*, 3384. (k) Süsse, L.; Hermeke, J.; Oestreich, M. *J. Am. Chem. Soc.* **2016**, *138*, 6940. (l) *Boronic acids*; Hall, D. G., Ed.; Wiley-VCH, Weinheim, **2005**. (m) Brown, H. C. *Boranes in Organic Chemistry*, Cornell University Press, Ithaca, 1972. (n) Suzuki, A. *Heterocycles*, **2010**, *80*, 15. (o) Campbell, P. G.; Marwitz, A. J. V.; Liu, S.-Y. *Angew. Chem. Int. Ed.* **2012**, *51*, 6074. (p) Bosdet, M. J. D.; Piers, W. E. *Can. J. Chem.* **2009**, *87*, 8. (q) Molander, G. A. *J. Org. Chem.* **2015**, *80*, 7837.

(6) (a) Rao, Y.-L.; Amarne, H.; Zhao,S.-B.; McCormick, T.M.; Martić, S.; Sun, Y.; Wang, R.-Y.; Wang, S. *J. Am. Chem. Soc.* **2008**, *130*, 12898. (b) Rao, Y.-L.; Amarne, H.; Wang, S. *Coord. Chem. Rev.* **2012**, *256*, 759. (c) Rao, Y.-L.; Hörl, C.; Braunschweig, H.; Wang, S. *Angew. Chem. Int. Ed.* **2014**, *53*, 9086. (d) Lu, J.-S.; Ko, S.-B.; Walters, N. R.; Kang, Y.; Sauriol, F.; Wang, S. *Angew. Chem. Int. Ed.* **2013**, *52*, 4544. (e) Ko, S.-B.; Lu, J.-S.; Wang, S. *Org. Lett.* **2014**, *16*, 616. (f) Yang, D.-T.; Mellerup, S. K.; Wang, X.; Lu, J.-S.; Wang, S. *Angew. Chem. Int. Ed.* **2015**, *54*, 5498.

(7) Wang, S.; Yang, D.-T.; Lu, J.; Shimogawa, H.; Gong, S.; Wang, X.; Mellerup, S. K.; Wakamiya, A.; Chang, Y.-L.; Yang, C.; Lu, Z. H. *Angew. Chem. Int. Ed.* **2015**, 54, 15074.

(8) (a) Paetzold, P.; Englert, U.; Finger, R.; Schmitz, T.; Tapper, A.; Ziembinski, R. *Z. Anorg. Allg. Chem.* **2004**, *630*, 508. (b) Hunold, R.; Pilz, M.; Allwohn, J.; Stadler, M.; Massa, W.; Schleyer, P. V. R.; Berndt, A. *Angew. Chem. Int. Ed. Engl.* **1989**, *28*, 781. (c) Pilz, M.; Stadler, M.; Hunold, R.; Allwohn, J.; Massa, W.; Berndt, A. *Angew. Chem. Int. Ed. Engl.* **1989**, *28*, 784. (d) Pilz, M.; Michel, H.; Berndt, A. *Angew. Chem. Int. Ed. Engl.***1990**, *29*, 401.

(9) (a) Klahn, M.; Rosenthal, U. *Organometallics* **2012**, *31*, 1235. (b) Caputo, C. B.; Hounjet, L. J.; Dobrovetsky, R.; Stephan, D. W. *Science*, **2013**, *341*, 1374. (c) Nair, N. G.; Mendoza-Cortes, J. L.; Abrol, R.; Goddard III, W. A.; Reddy, V. P. *J. Organomet. Chem.* **2013**, *747*, 133.

(10) (a) Polli, D.; Altoe, P.; Weingart, O.; Spillane, K. M.; Manzoni, C.; Brida, D.; Tomasello, G.; Orlandi, G.; Kukura, P.; Mathies, R. A.; Garavelli, M.; Cerullo, G. *Nature* **2010**, *467*, 440. (b) Blancafort, L. *ChemPhysChem* **2014**, *15*, 3166.

(11) Iida, A.; Saito, S.; Sasamori, T.; Yamaguchi, S. *Angew. Chem. Int. Ed.* **2013**, *52*, 3760.

(12) (a) Zhang, Z.; Edkins, R. M.; Haehnel, M.; Wehner, M.; Eichhorn, A.; Mailänder, L.; Meier, M.; Brand, J.; Brede, F.; Müller-Buschbaum, K.; Braunschweig, H.; Marder, T. B. *Chem. Sci.* **2015**, *6*, 5922. (b) Yin, X.; Chen, J.; Lalancette, R. A.; Marder, T. B.; Jäkle, F. *Angew. Chem. Int. Ed.* **2014**, *53*, 9761.

SYNOPSIS TOC